している。

C. 研究結果

生活習慣病・難治性疾患関連遺伝子に関するENUミュータジェネシスによる約1600匹分のラットミュータントアーカイブの高速DNAスクリーニングの結果レプチンおよびセイピン遺伝子に変異を有するラットの同定に成功し、さらに独自開発した個体復元技術ICSIを用いて標的遺伝子変異ラット系統樹立に成功し、糖脂質代謝、膵分泌能を中心に表現系解析を行った。その結果、レプチン遺伝子ナンセンス変異ラットでは明らかな肥満と摂食量の亢進をみとめた。レプチン遺伝子ナンセンス変異ラットに糖負荷試験を行った結果、血中グルコース濃度高値、高インスリン血症を認め、耐糖能の異常、インスリン抵抗性の存在が確認された。また、中性脂肪高値、遊離脂肪酸高値、総コレステロール値高値などの脂質異常も見出された。また、レプチン遺伝子ナンセンス変異ラットの膵臓では、ラ氏島の拡大を認め、beta細胞などの肥大が考えられた。本変異ラットの膵頭におけるGPR40、Pdx1の遺伝子発現を検討したところ、いずれも約50%に低下していた。このことから本レプチン遺伝子変異ラットの食後高血糖、インスリン初期分泌低下にこれら遺伝子産物の発現低下が関与する可能性が示唆された。一方、脂肪委縮症の原因遺伝子であるセイピン遺伝子の変異ラットの解析も行い、ヒト脂肪委縮症に類似した脂肪減少、脂肪肝、糖代謝異常を認めた。今後、更に詳細な解析を継続していく予定である。

D. 考察

生活習慣病関連疾患の病態解明においては複数の臓器における病態の同時進行的変化とそれに伴う液性因子を介した臓器間シグナルクロストーク解明が必須であり、またこれら病態には細胞老化も関与するため、その治療において細胞・臓器再生という観点も不可欠である。現在これら疾患の病態解析、創薬開発、再生医療研究には遺伝子改変技術が確立されているマウスがモデル動物として多く用いられているが、マウスはその小ささゆえに採血や組織採取が困難であること、生理学的解析や移植実験が行ないにくいなどの問題がある。そのため、マウスと比べ体のサイズが大きく、採血や組織採取や系統的な生理学的解析が容易で、移植実験も行ないやすく、代謝面でもよりヒトに近いラットでの疾患モデル確立が期待されている。実際今回得られたレプチンおよびセイピン遺伝子変異ラットにおいて代謝パラメーターの解析においてより安定した結果を得られること、また、膵組織の詳細な組織学的解析および分子生物学的解析が可能であることが確認された。今後その表現系を、さらに詳細に解析することにより、これら遺伝子変異ラットのモデル動物としての意義が確立されれば、病態解明・新規治療標的同定および新規創薬開発への応用を進めていきたい。

E. 結論

生活習慣病・難治性疾患関連遺伝子に関して、複数の糖尿病、メタボリックシンドローム関連遺伝子変異ラットの同定、系統樹立に成功し、その中でレプチンおよびセイピン遺伝子変異ラットの表現系、特に糖代謝および膵島の遺伝子発現の解析を行い、本遺伝子変異ラットのモデル動物としての有用性を示した。今後これら遺伝子変異ラットの表現系解析をさらに継続し、疾患モデルラットとしての意義を確立し、病態解明・新規治療標的同定と新規創薬開発への応用を進めていきたい。

F. 健康危険情報

なし

G. 研究発表

1. 論文発表

1. M. Zhao, Y. Li, J. Wang, K. Ebihara, X. Rong, K. Hosoda, T. Tomita, K. Nakao.
Azilsartan treatment improves insulin sensitivity in obese spontaneously hypertensive Koletsky rats.
Diabetes Obes Metab.13(12) 1123-1129. 2011.

2. Aizawa-Abe M, Ebihara K, Ebihara C, Mashimo T, Takizawa A, Tomita T, Kusakabe T, Yamamoto Y, Aotani D, Yamamoto-Kataoka S, Sakai T, Hosoda K, Serikawa T, Nakao K.

Generation of leptin-deficient Lepmkyo/Lepmkyo rats and identification of leptin-responsive genes in the liver.
Physiol Genomics. 45(17):786-93.2013

3. Odori S, Hosoda K, Tomita T, Fujikura J, Kusakabe T, Kawaguchi Y, Doi R, Takaori K, Ebihara K, Sakai Y, Uemoto S, Nakao K. GPR119 expression in normal human tissues and islet cell tumors: evidence for its islet-gastrointestinal distribution, expression in pancreatic beta and alpha cells, and involvement in islet function.
Metabolism. 62(1):70-8.2013

4. Tomita T, Hosoda K, Fujikura J, Inagaki N, Nakao K.
The G-Protein-Coupled Long-Chain Fatty Acid Receptor GPR40 and Glucose Metabolism.
Front Endocrinol (Lausanne). 2014. 5:152.

2. 学会発表

国際学会

1. T. Tomita, K. Hosoda, S. Odori, Y. Kira, C. Son, J. Fujikura, H. Iwakura, M. Noguchi, E. Mori, M. Naito, T. Kusakabe, K. Ebihara, K. Nakao
Gene Expression of a G Protein-coupled Receptor, GPR40, in Pancreatic Islets of a Genetically Obese Rat Model
Keystone Symposia (Killarney, Co. Kerry, Ireland) May 15-20, 2011

国内学会

1. 冨田努, 細田公則, 小鳥真司, 藤倉純二, 岩倉浩, 野口倫生, 森栄作, 内藤雅喜, 日下部徹, 海老原健, 中尾一和
新規のインスリン分泌調節因子 GPR40 の遺伝子肥満モデルでの発現調節
第 84 回日本内分泌学会学術総会、2011. 4. 21-23、神戸

2. 野村英生, 孫徹, 後藤伸子, 勝浦五郎, 野口倫生, 冨田努, 藤倉純二, 海老原健, 細田公則, 中尾一和
高脂肪食負荷マウス中枢におけるレプチン反応性の経時的変化の検討
第 84 回日本内分泌学会学術総会、2011. 4. 21-23、神戸

3. 小鳥真司, 冨田努, 孫徹, 藤倉純二, 野口倫生, 森栄作, 内藤雅喜, 日下部徹, 海老原健, 細田公則, 中尾一和
新規の G 蛋白共役型-脂質受容体 GPR119 の臨床的意義：ヒトおよびマウスでの膵島における遺伝子発現と膵島機能との連関
第 84 回日本内分泌学会学術総会、2011. 4. 21-23、神戸

4. 阿部恵, 海老原健, 海老原千尋, 宮澤崇, 冨田努, 日下部徹, 山本祐二, 宮本理人, 真下知士, 細田公則, 芹川忠夫, 中尾一和
糖脂質代謝におけるレプチンの病態生理的意義に関する種族差の検討—レプチン欠損 ob/ob ラットの開発と解析—
第 84 回日本内分泌学会学術総会 2011. 4. 21-23、神戸

5. 内藤雅喜, 藤倉純二, 森栄作, 小鳥真司, 野口倫生, 冨田努, 孫徹, 日下部徹, 宮永史子, 宮本理人, 山本祐二, 海老原健, 細田公則, 中尾一和
Leptin Transgenic Akita mouse を用いたインスリン分泌低下型糖尿病に対するレプチン治療
第 84 回日本内分泌学会学術総会 2011. 4. 21-23、神戸

6. 井田みどり, 桝田出, 細田公則, 海老原健, 藤倉純二, 岩倉浩, 日下部徹, 山本祐二, 阿部恵, 冨田努, 葛谷英嗣, 中尾一和
Dual Bioimpedance 法を用いた内臓脂肪量測定装置のスクリーニング機器としての有用性
第 84 回日本内分泌学会学術総会 2011. 4. 21-23、神戸

7. 冨田努, 細田公則, 小鳥真司, 孫徹, 藤倉純二, 岩倉浩, 野口倫生, 森栄作, 内藤雅喜, 吉良友里, 日下部徹, 海老原健, 益崎裕章, 中尾一和
膵β細胞に高発現し、中・長鎖脂肪酸をリガンドする G 蛋白共役型受容体 GPR40 の遺伝性肥満モデルの膵島での発現調節
第 54 回日本糖尿病学会年次学術集会、

2011. 5. 19-21、札幌

8. 阿部恵, 海老原健, 海老原千尋, 宮澤崇, 冨田努, 日下部徹, 山本祐二, 宮本理人, 真下知士, 細田公則, 芹川忠夫, 中尾一和
レプチン欠損ob/obラットの開発と糖脂質代謝解析
第 54 回日本糖尿病学会年次学術集会、2011. 5. 19-21、札幌

9. 野口倫生, 冨田努, 孫徹, 日下部徹, 宮永史子, 宮本理人, 山本祐二, 海老原健, 細田公則, 中尾一和
Leptin Transgenic Akita マウスを用いたインスリン分泌低下型糖尿病に対するレプチン治療
第 54 回日本糖尿病学会年次学術集会、2011. 5. 19-21、札幌

10. 細田公則, 井田みどり, 桝田出, 海老原健, 藤倉純二, 岩倉浩, 日下部徹, 山本祐二, 阿部恵, 冨田努, 葛谷英嗣, 中尾一和
Dual Bioimpedance 法を用いた内臓脂肪量測定装置のスクリーニング機器としての有用性
第 54 回日本糖尿病学会年次学術集会、2011. 5. 19-21、札幌

11. 野村英生, 孫徹, 野口倫生, 冨田努, 藤倉純二, 海老原健, 細田公則, 中尾一和
高脂肪食負荷レプチン抵抗モデルマウスにおける部位特異的レプチン反応性の検討
第 54 回日本糖尿病学会年次学術集会、2011. 5. 19-21、札幌

12. 小鳥真司, 冨田努, 孫徹, 藤倉純二, 野口倫生, 森栄作, 内藤雅喜, 日下部徹, 海老原健, 細田公則, 中尾一和
新規の G 蛋白共役型-脂質受容体 GPR119 の臨床的意義：ヒトおよびマウスでの膵島における遺伝子発現と膵島機能との連関
第 54 回日本糖尿病学会年次学術集会、2011. 5. 19-21、札幌

13. 冨田努, 細田公則, 小鳥真司, 孫 徹, 藤倉純二, 岩倉浩, 野口倫生, 日下部徹, 海老原健, 中尾一和
G 蛋白共役型-脂肪酸受容体 GPR40 の遺伝性肥満モデルの膵島での発現調節
第 32 回日本肥満学会 学術集会、2011.9.23-24、兵庫県淡路島

14. 孫 徹, 野村英生, 後藤伸子, 勝浦五郎, 野口倫生, 冨田努, 藤倉純二, 海老原健, 細田公則, 中尾一和
高脂肪食負荷レプチントランスジェニックマウス中枢におけるレプチン反応性の検討
第 32 回日本肥満学会 学術集会、2011.9.23-24、兵庫県淡路島

15. 内藤雅喜, 藤倉純二, 森栄作, 野口倫生, 冨田努, 孫 徹, 日下部徹, 海老原健, 細田公則, 中尾一和
Leptin Transgenic Akita mouse を用いたインスリン分泌低下型糖尿病に対するレプチン治療
第 32 回日本肥満学会 学術集会、2011.9.23-24、兵庫県淡路島

16. 小鳥真司, 冨田努, 孫 徹, 藤倉純二, 野口倫生, 森栄作, 内藤雅喜, 日下部徹, 海老原健, 細田公則,中尾一和
G 蛋白共役型-脂肪酸受容体 GPR40 の遺伝性肥満モデルの膵島での発現調節
第 32 回日本肥満学会 学術集会、2011.9.23-24、兵庫県淡路島

17. 内藤雅喜, 藤倉純二, 森栄作, 小鳥真司, 野村英生、孫徹、後藤伸子、勝浦五郎、野口倫生、冨田努、藤倉純二、海老原健、細田公則、中尾一和
高脂肪食負荷レプチントランスジェニック(LepTg)マウスにおけるレプチン感受性の検討
第 34 回日本肥満学会、2013.10.11-12、東京都

18. 冨田努、細田公則、小鳥真司、藤倉純二、海老原健、中尾一和
膜型脂質受容体 GPR40 の遺伝性肥満 Koletsky ラット膵島での発現調節とその意義
第 34 回日本肥満学会、2013.10.11-12、東京都

19. 山下貴裕、森栄作、藤倉純二、野口倫生、冨田努、孫徹、横井秀基、日下部徹、海老原健、細田公則、中尾一和
腎性浮腫との鑑別を要した Lipoedema の一例
第 34 回日本肥満学会、2013.10.11-12、東京都

20. 冨田努
G 蛋白共役型—脂肪酸受容体 GPR40 の肥満・糖尿病での発現調節と意義
第 50 回日本糖尿病学会近畿地方会・第 49 回日本糖尿病協会近畿地方会, 2013.11.23, 京都市

21. 小鳥真司、冨田努、藤倉純二、日下部徹、海老原健、細田公則、河野茂夫、中尾一和
G 蛋白共役型－脂質受容体 GPR119 の臨床的意義：ヒトの膵島および膵島細胞腫瘍における遺伝子発現と膵島機能との連関
第 56 回日本糖尿病学会年次学術集会、2013.5.16-18、熊本

22. 冨田努、細田公則、小鳥真司、藤倉純二、日下部徹、海老原健、中尾一和
G 蛋白共役型－脂肪酸受容体 GPR40 の糖尿病における発現調節と意義
第 56 回日本糖尿病学会年次学術集会、2013.5.16-18、熊本

23. 内藤雅喜、藤倉純二、野口倫生、冨田努、日下部徹、孫徹、海老原健、細田公則、中尾一和
1 型糖尿病モデルマウスにおける高レプチン血症の影響
第 56 回日本糖尿病学会年次学術集会、2013.5.16-18、熊本

24. 吉良友里、冨田努、細田公則、藤倉純二、海老原千尋、阿部恵、海老原健、中尾一和、稲垣暢也
新規の遺伝性肥満モデル *mkyo/mkyo* ラット膵島における脂質受容体 GPR40 の遺伝子発現調節
第 88 回日本内分泌学会学術総会、2014.4.23-25、仙台国際センター

25. 吉良友里、冨田努、細田公則、藤倉純二、海老原千尋、阿部　恵、海老原健、中尾一和、稲垣暢也
新規の遺伝性肥満モデル *mkyo/mkyo* ラット膵島における脂質受容体 GPR40 の遺伝子発現調節
第 58 回日本糖尿病学会年次学術集会、2015.5.21-24、山口県下関市

H. 知的財産権の出願・登録状況
なし

研究成果の刊行に関する一覧表

雑誌

発表者氏名	論文タイトル名	発表誌名	巻号	ページ	出版年
Ogawa, Y., Mukoyama, M., Yokoi, H., Kasahara, M., Mori, K., Kato, Y., Kuwabara, T., Imamaki, H., Kawanishi, T., Koga, K., Ishii, A., Tokudome, T., Kishimoto, I., Sugawara, A., Nakao, K.	Natriuretic peptide receptor guanylyl cyclase-A protects podocytes from aldosterone-induced glomerular injury.	J Am Soc Nephrol	23	1198-209	2012
Minami T, Kuwahara K, Nakagawa Y, Takaoka M, Kinoshita H, Nakao K, Kuwabara Y, Yamada Y, Yamada C, Shibata J, Usami S, Yasuno S, Nishikimi T, Ueshima K, Sata M, Nakano H, Seno T, Kawahito Y, Sobue K, Kimura A, Nagai R, Nakao K.	Reciprocal expression of MRTF-A and myocardin in crucial for pathological vascular remodelling in mice.	EMBO J	31	4428-40	2012
Yokoi, H., Kasahara, M., Mori, K., Ogawa, Y., Kuwabara, T., Imamaki, H., Kawanishi, T., Koga, K., Ishii, A., Kato, Y., Mori, P. K., Toda, N., Ohno, S., Muramatsu, H., Muramatsu, T., Sugawara, A., Mukoyama, M., and Nakao, K.	Pleiotrophin triggers inflammation and increased peritoneal permeability leading to peritoneal fibrosis.	Kidney Int	81	160-9	2012
Kuwabara, T., Mori, K., Mukoyama, M., Kasahara, M., Yokoi, H., Saito, Y., Ogawa, Y., Imamaki, H., Kawanishi, T., Ishii, A, Koga, K., Mori, PK., Kato, Y., Sugawara, A., Nakao, K.	Exacerbation of diabetic nephropathy by hyperlipidaemia is mediated by toll-like receptor 4 in mice.	Diabetologia	81	2256-66	2012
L. Miyamoto, K. Ebihara, T. Kusakabe, D. Aotani, S. Yamamoto-Kataoka, T. Sakai, M. Aizawa-Abe, Y. Yamamoto, J. Fujikura, T. Hayashi, K. Hosoda, K. Nakao.	Leptin activates hepatic 5' AMP-Activated Protein Kinase through sympathetic nervous system and α1 adrenergic receptor: A potential mechanism for improvement of fatty liver in lipodystrophy by leptin.	J Biol Chem	287	40441-7	2012
M. Iwanishi, K. Ebihara, T. Kusakabe, S. Harada, J. Ito-Kobayashi, A. Tsuji, K. Hosoda, K. Nakao K.	Premature atherosclerosis in a Japanese diabetic patient with atypical familial partial lipodystrophy and hypertriglyceridemia.	Intern Med	51	2573-9	2012
D. Aotani, K. Ebihara, N. Sawamoto, T. Kusakabe, M. Aizawa-Abe, S. Kataoka, T. Sakai, H. Iogawa, C. Ebihara, J. Fujikura, K. Hosoda, H. Fukuyama, K. Nakao.	Functional Magnetic Resonance Imaging Analysis of Food-Related Brain Activity in Patients with Lipodystrophy Undergoing Leptin Replacement Therapy.	J Clin Endocrinol Metab	97	3663-71	2012

N. Yamada-Goto, G. Katsuura, Y. Ochi, K. Ebihara, T. K usakabe, K. Hosoda, K. Nakao.	Impairment of fear-conditioning responses and changes of brain neurotrophic factors in diet-induced obese mice.	J Neuroendocrinol	24	1120-5	2012
T. Kusakabe, K. Ebihara, T. Sakai, L. Miyamoto, D. Aota ni, Y. Yamamoto, S. Yamamoto-Kataoka, M. Aizawa-Abe, J. Fujikura, K. Hosoda, K. Nakao.	Amylin improves the effect of leptin on insulin sensitivity in leptin-resistant diet-induced obese mice.	Am J Physiol Endocrinol Metab	302	E924-31	2012
Yokoi, H., Kasahara, M., Mori, K., Kuwabara, T., Toda, N., Yamada, R., Namoto, S., Yamamoto, T., Seki, N., So uma, N., Yamaguchi, T., Sugawara, A., Mukoyama, M., a nd Nakao, K.	Peritoneal fibrosis and high transpoare induced in mildly pre-injured peritoneum by 3,4-dideoxyglucosone-3-ene in mice.	Perit Dial Int	33	143-54	2013
Nishikimi T, Okamoto H, Nakamura M, Ogawa N, Horii K, Nagata K, Nakagawa Y, Kinoshita H, Yamada C, Nak ao K, Minami T, Kuwabara Y, Kuwahara K, Masuda I, Kangawa K, Minamino N, Nakao K.	Direct immunochemiluminescent assay for proBNP and total BNP in human plasma proBNP and total BNP levels in normal and heart failure	PLoS One	8	e53233	2013
Nishikimi T, Kuwahara K, Nakagawa Y, Kangawa K, Min amino N, Nakao K.	Complexity of melicular forms of B-type natriuretic peptide in heart failure.	Heart	99	677-9	2013
Hitomi T, Habu T, Kobayashi H, Okuda H, Harada KH, Osafune K, Taura D, Sone M, Asaka I, Ameku T, Watan abe A, Kasahara T, Sudo T, Shiota F, Hashikata H, Taka gi Y, Morito D, Miyamoto S, Nakao K, Koizumi A.	The moyamoya disease susceptibility variant RNF213 R4810K (rs112735431) induces genomic instability by mitotic abnormality	Biochem Biophys Res Commun	439	419-26	2013
Hitomi T, Habu T, Kobayashi H, Okuda H, Harada KH, Osafune K, Taura D, Sone M, Asaka I, Ameku T, Watan abe A, Kasahara T, Sudo T, Shiota F, Hashikata H, Taka gi Y, Morito D, Miyamoto S, Nakao K, Koizumi A.	Downregulation of Securin by the variant RNF213 R4810K (rs112735431, G>A) reduces angiogenic activity of induced pluripotent stem cell-derived vascular endothelial cells from moyamoya patients.	Biochem Biophys Res Commun	438	13-9	2013
Honda K, Sone M, Tamura N, Sonoyama T, Taura D, Ko jima K, Fukuda Y, Tanaka S, Yasuno S, Fujii T, Kinoshi ta H, Ariyasu H, Kanamoto N, Miura M, Yasoda A, Arai H, Ueshima K, Nakao K.	Adrenal reserve function after unilateral adrenalectomy in patients with primary aldosteronism.	J Hypertens	31	2010-7	2013
Aizawa-Abe M, Ebihara K, Ebihara C, Mashimo T, Takiz awa A, Tomita T, Kusakabe T, Yamamoto Y, Aotani D, Yamamoto-Kataoka S, Sakai T, Hosoda K, Serikawa T, N akao K.	Generation of leptin-deficient Lepmkyo/Lepmkyo rats and identification of leptin-responsive genes in the liver.	Physiol Genomics	45	786-93	2013

Noguchi M, Hosoda K, Nakane M, Mori E, Nakao K, Ta ura D, Yamamoto Y, Kusakabe T, Sone M, Sakurai H, F ujikura J, Ebihara K, Nakao K.	In vitro characterization and engraftment of adipocytes derived from human induced pluripotent stem cells and embryonic stem cells. .	Stem Cells Dev	22	2895-905	2013
Fujikura J, Hosoda K, Nakao K	Cell transplantation therapy for diabetes mellitus: endocrine pancreas and adipocyte.	Endocr J	60	697-708	2013
Kitamoto A, Kitamoto T, Mizusawa S, Teranishi H, So R, Matsuo T, Nakata Y, Hyogo H, Ochi H, Nakamura T, Kamohara S, Miyatake N, Kotani K, Komatsu R, Itoh N, Mineo I, Wada J, Yoneda M, Nakajima A, Funahashi T, Miyazaki S, Tokunaga K, Masuzaki H, Ueno T, Chaya ma K, Hamaguchi K, Yamada K, Hanafusa T, Oikawa S, Sakata T, Tanaka K, Matsuzawa Y, Nakao K, Sekine A, Hotta K.	NUDT3 rs206936 is associated with body mass index in obese Japanese women.	Endocr J	60	991-1000	2013
Ida M, Hirata M, Odori S, Mori E, Kondo E, Fujikura J, Kusakabe T, Ebihara K, Hosoda K, Nakao K.	Early changes of abdominal adiposity detected with weekly dual bioelectrical impedance analysis during calorie restriction.	Obesity	21	E350-3	2013
Bando M, Iwakura H, Ariyasu H, Koyama H, Hosoda K, Adachi S, Nakao K, Kangawa K, Akamizu T.	Overexpression of intraislet ghrelin enhances β-cell proliferation after streptozotocin-induced β-cell injury in mice.	Am J Physiol Endocrinol Metab	305	E140-8	2013
Uosaki H, Magadum A, Seo K, Fukushima H, Takeuchi A, Nakagawa Y, Moyes KW, Narazaki G, Kuwahara K, Laflamme M, Matsuoka S, Nakatsuji N, Nakao K, Kwon C, Kass DA, Engel FB, Yamashita JK..	Identification of Chemicals Inducing Cardiomyocyte Proliferation in Developmental Stage-Specific Manner with Pluripotent Stem Cells.	Circ Cardiovasc Genet	6	624-33	2013
Yasuno S, Kuwahara K, Kinoshita H, Yamada C, Nakaga wa Y, Usami S, Kuwabara Y, Ueshima K, Harada M, Ni shikimi T, Nakao K.	Angiotensin II Type 1a receptor signaling directly contributes to the increased arrhythmogenicity in cardiac hypertrophy	Br J Pharmacol	170	1384-95	2013

Nishikimi T, Kuwahara K, Nakagawa Y, Kangawa K, Na kao K.	Adrenomedullin in Cardiovascular Disease: A Useful Biomarker, Its Pathological Roles and Therapeutic Application.	Curr Protein Pept Sci	14	256-67	2013
Kuwabara Y, Kuwahara K, Takano M, Kinoshita H, Arai Y, Yasuno S, Nakagawa Y, Igata S, Usami S, Minami T, Yamada Y, Nakao K, Yamada C, Shibata J, Nishikimi T, Ueshima K, Nakao K.	Increased Expression of HCN Channels in the Ventricular Myocardium Contributes to Enhanced Arrhythmicity in Mouse Failing Hearts.	J Am Heart Assoc	2	E000150	2013
Funayama A, Shishido T, Netsu S, Narumi T, Kadowaki S, Takahashi H, Miyamoto T, Watanabe T, Woo CH, Ab e JI, Kuwahara K, Nakao K, Takeishi Y, Kubota I	Cardiac nuclear High Mobility Group Box 1 prevents the development of cardiac hypertrophy and heart failure.	Cardiovasc Res	99	657-64	2013
Nishikimi T, Okamoto H, Nakamura M, Ogawa N, Horii K, Nagata K, Nakagawa Y, Kinoshita H, Yamada C, Nak ao K, Minami T, Kuwabara Y, Kuwahara K, Masuda I, Kangawa K, Minamino N, Nakao K.	Direct Immunochemiluminescent Assay for proBNP and Total BNP in Human Plasma proBNP and Total BNP Levels in Normal and Heart Failure.	PLoS One	8	E53233	2013
Matsumoto E, Sasaki S, Kinoshita H, Kito T, Ohta H, Ko nishi M, Kuwahara K, Nakao K, Itoh N	Angiotensin II-induced cardiac hypertrophy and fibrosis are promoted in mice lacking Fgf16.	Genes Cells	18	544-53	2013
Kitamoto T, Kitamoto A, Yoneda M, Hyogo H, Ochi H, Nakamura T, Teranishi H, Mizusawa S, Ueno T, Chayam a K, Nakajima A, Nakao K, Sekine A, Hotta K.	Genome-wide scan revealed that polymorphisms in the PNPLA3, SAMM50, and PARVB genes are associated with development and progression of nonalcoholic fatty liver disease in Japan.	Hum Genet	132	783-92	2013
Sone M, Nakao K	Vascular research using human pluripotent stem cells and humoral factors	Endocr J	60	397-402	2013
Yamada-Goto N, Katsuura G, Ebihara K, Inuzuka M, Ochi Y, Yamashita Y, Kusakabe T, Yasoda A, Satoh-Asahara N, Ariyasu H, Hosoda K, Nakao K.	Intracerebroventricular administration of C-type natriuretic peptide suppresses food intake via activation of the melanocortin system in mice.	Diabetes	62	1500-4	2013

Hotta K, Kitamoto A, Kitamoto T, Mizusawa S, Teranishi H, So R, Matsuo T, Nakata Y, Hyogo H, Ochi H, Nakamura T, Kamohara S, Miyatake N, Kotani K, Itoh N, Mineo I, Wada J, Yoneda M, Nakajima A, Funahashi T, Miyazaki S, Tokunaga K, Masuzaki H, Ueno T, Chayama K, Hamaguchi K, Yamada K, Hanafusa T, Oikawa S, Sakata T, Tanaka K, Matsuzawa Y, Nakao K, Sekine A.	Replication study of 15 recently published Loci for body fat distribution in the Japanese population.	J Atheroscler Thromb	20	336-50	2013
Sakai T, Kusakabe T, Ebihara K, Aotani D, Yamamoto-Kataoka S, Zhao M, Gumbilai VM, Ebihara C, Aizawa-Abe M, Yamamoto Y, Noguchi M, Fujikura J, Hosoda K, Inagaki N, Nakao K	Leptin restores the insulinotropic effect of exenatide in a mouse model of type 2 diabetes with increased adiposity induced by streptozotocin and high-fat diet.	Am J Physiol Endocrinol Metab	307	E712-719	2014
Tanaka M, Yamaguchi S, Yamazaki Y, Kinoshita H, Kuwahara K, Nakao K, Jay PY, Noda T, Nakamura T.	Somatic chromosomal translocation between *Ewsr1* and *Fli1* loci leads to dilated cardiomyopathy in a mouse model	Sci Rep	5	7826	2015
Oshita K, Itoh M, Hirashima S, Kuwabara Y, Ishihara K, Kuwahara K, Nakao K, Kimura T, Nakamura K, Ushijima K, Takano M.	Ectopic automaticity induced in ventricular myocytes by transgenic overexpression of HCN2	J Mol Cell Cardiol	80	81-89	2015
Yamada Y, Kinoshita H, Kuwahara K, Nakagawa Y, Kuwabara Y, Minami T, Yamada C, Shibata J, Nakao K, Cho K, Arai Y, Yasuno S, Nishikimi T, Ueshima K, Kamakura S, Nishida M, Kiyonaka S, Mori Y, Kimura T, Kangawa K, Nakao K	Inhibition of N-type Ca^{2+} channels ameliorates an imbalance in cardiac autonomic nerve activity and prevents lethal arrhythmias in mice with heart failure	Cardiovascular Research	104	183-93	2014
Nakagawa Y, Nishikimi T, Kuwahara K, Yasuno S, Kinoshita H, Kuwabara Y, Nakao K, Minami T, Yamada C, Ueshima K, Ikeda Y, Okamoto H, Horii K, Nagata K, Kangawa K, Minamino N, Nakao K.	The Effects of Super-Flux (High Performance) Dialyzer on Plasma Glycosylated Pro-B-Type Natriuretic Peptide (proBNP) and Glycosylated N-Terminal proBNP in End-Stage Renal Disease Patients on Dialysis	PLoS One	9	e92314	2014

Kuwabara T, Mori K, Mukoyama M, Kasahara M, Yokoi H, Nakao K	Macrophage-mediated glucolipotoxicity via myeloid-related protein 8/toll-like receptor 4 signaling in diabetic nephropathy	Clin Exp Nephrol	18	584-592	2014
Kuwabara T, Mori K, Kasahara M, Yokoi H, Imamaki H, Ishii A, Koga K, Sugawara A, Yasuno S, Ueshima K, Morikawa T, Konishi Y, Imanishi M, Nishiyama A, Nakao K, Mukoyama M.	Predictive significance of kidney myeloid-related protein 8 expression in patients with obesity- or type 2 diabetes-associated kidney diseases.	PLoS One	9	e88942	2014
Tomita T, Hosoda K, Fujikura J, Inagaki N, Nakao K.	The G-Protein-Coupled Long-Chain Fatty Acid Receptor GPR40 and Glucose Metabolism.	Front Endocrinol	5	152	2014
Kanda J, Mori K, Kawabata H, Kuwabara T, Mori KP, Imamaki H, Kasahara M, Yokoi H, Mizumoto C, Thoennissen NH, Koeffler HP, Barasch J, Takaori-Kondo A, Mukoyama M, Nakao K.	An AKI biomarker lipocalin 2 in the blood derives from the kidney in renal injury but from neutrophils in normal and infected conditions.	Clin Exp Nephrol	19	99-106	2014
Ebihara C, Ebihara K, Aizawa-Abe M, Mashimo T, Tomita T, Zhao M, Gumbilai V, Kusakabe T, Yamamoto Y, Aotani D, Yamamoto-Kataoka S, Sakai T, Hosoda K, Serikawa T, Nakao K.	Seipin is necessary for normal brain development and spermatogenesis in addition to adipogenesis.	Hum Mol Genet		In press	2015

BASIC RESEARCH www.jasn.org

Natriuretic Peptide Receptor Guanylyl Cyclase-A Protects Podocytes from Aldosterone-Induced Glomerular Injury

Yoshihisa Ogawa,* Masashi Mukoyama,* Hideki Yokoi,* Masato Kasahara,* Kiyoshi Mori,* Yukiko Kato,* Takashige Kuwabara,* Hirotaka Imamaki,* Tomoko Kawanishi,* Kenichi Koga,* Akira Ishii,* Takeshi Tokudome,† Ichiro Kishimoto,‡ Akira Sugawara,* and Kazuwa Nakao*

*Department of Medicine and Clinical Science, Kyoto University Graduate School of Medicine, Kyoto, Japan; †Department of Biochemistry, National Cerebral and Cardiovascular Research Institute, Osaka, Japan; and ‡Department of Atherosclerosis and Diabetes, National Cerebral and Cardiovascular Center, Osaka, Japan

ABSTRACT

Natriuretic peptides produced by the heart in response to cardiac overload exert cardioprotective and renoprotective effects by eliciting natriuresis, reducing BP, and inhibiting cell proliferation and fibrosis. These peptides also antagonize the renin-angiotensin-aldosterone system, but whether this mechanism contributes to their renoprotective effect is unknown. Here, we examined the kidneys of mice lacking the guanylyl cyclase-A (GC-A) receptor for natriuretic peptides under conditions of high aldosterone and high dietary salt. After 4 weeks of administering aldosterone and a high-salt diet, GC-A knockout mice, but not wild-type mice, exhibited accelerated hypertension with massive proteinuria. Aldosterone-infused GC-A knockout mice had marked mesangial expansion, segmental sclerosis, severe podocyte injury, and increased oxidative stress. Reducing the BP with hydralazine failed to lessen such changes; in contrast, blockade of the renin-angiotensin-aldosterone system markedly reduced albuminuria, ameliorated podocyte injury, and reduced oxidative stress. Furthermore, treatment with the antioxidant tempol significantly reduced albuminuria and abrogated the histologic changes. In cultured podocytes, natriuretic peptides inhibited aldosterone-induced mitogen-activated protein kinase phosphorylation. Taken together, these results suggest that renoprotective properties of the endogenous natriuretic peptide/GC-A system may result from the local inhibition of the renin-angiotensin-aldosterone system and oxidative stress in podocytes.

J Am Soc Nephrol 23: 1198–1209, 2012. doi: 10.1681/ASN.2011100985

Aldosterone, beyond its effects on sodium reabsorption, has been shown to play an important role in causing cardiovascular complications including renal injury.[1,2] Proteinuria is not rare in patients with primary aldosteronism, suggesting that aldosterone can induce renal injury independent of circulating angiotensin II (AngII) levels.[3] In experimental nephropathy models, aldosterone exerts direct effects on renal cells, leading to the progression of glomerulosclerosis and proteinuria.[4] Several studies have revealed positive feedback by which aldosterone activates the renin-angiotensin-aldosterone system (RAAS), through inducing renin and angiotensin-converting enzyme gene expression,[5,6] or by activating AngII type 1 (AT1) receptor signaling.[7] Furthermore, aldosterone upregulates reactive oxygen species (ROS) and activates mitogen-activated protein kinases (MAPKs) in the kidney and cardiovascular system.[7–9]

Podocytes play a crucial role in barrier function as well as the pathogenesis of glomerular diseases, forming a branched interdigitating network with foot processes by the slit diaphragm.[10] Genetic

Received October 13, 2011. Accepted April 15, 2012.

Published online ahead of print. Publication date available at www.jasn.org.

Correspondence: Dr. Masashi Mukoyama, Department of Medicine and Clinical Science, Kyoto University Graduate School of Medicine, 54 Shogoin Kawahara-cho, Sakyo-ku, Kyoto 606-8507, Japan. Email: muko@kuhp.kyoto-u.ac.jp

studies have proved roles of slit diaphragm–associated proteins, including nephrin and podocin, in various proteinuric disorders.[10] Recently, podocytes have attracted greater attention as the target for aldosterone action. In fact, aldosterone causes foot process effacement and downregulation of nephrin and podocin, via the mineralocorticoid receptor.[7,11–13] In addition, the mineralocorticoid receptor in podocytes can be activated by Rac1 GTPase, which is sufficient to cause glomerular injury and proteinuria irrespective of aldosterone levels.[13]

The natriuretic peptide family consisting of atrial natriuretic peptide (ANP), brain natriuretic peptide (BNP), and C-type natriuretic peptide possess potent diuretic, natriuretic, and vasodilating properties.[14] ANP and BNP are secreted predominantly by the cardiac atrium and ventricle, respectively, upon cardiac overload.[14–16] They exert various biologic effects by acting on guanylyl cyclase-A (GC-A)/natriuretic peptide receptor-A (NPR-A), which is the major and possibly the only receptor for ANP and BNP, through the activation of cGMP/cGMP-dependent protein kinase.[17] GC-A is abundantly expressed in blood vessels and the heart[17]; within the kidney, it is localized in glomeruli, thin limbs of Henle's loop, cortical collecting ducts, and inner medullary collecting ducts.[18] In glomeruli, GC-A is expressed in mesangial cells and podocytes.[18] GC-A–deficient mice show chronic salt-independent elevation of BP by approximately 15–30 mmHg[19] and cardiac hypertrophy,[20] with virtually no natriuretic or diuretic response to acute volume expansion.[21] These studies clearly demonstrate essential roles for natriuretic peptide/GC-A signaling in BP regulation and acute volume handling through the kidney, but the role of GC-A in podocyte injury remains elusive.

A renoprotective action of ANP has been shown early using animal models of ARF.[22] A recent meta-analysis reveals that the administration of low-dose ANP may exert beneficial effects in clinical AKI.[23] We previously showed that chronic excess of BNP in mice prevents glomerular injury after subtotal nephrectomy,[24] and ameliorates proteinuria and histologic changes in immune-mediated renal injury[25] as well as in diabetic nephropathy.[26] In addition to exerting direct vasodilating and diuretic actions, natriuretic peptides act to antagonize the RAAS at multiple steps.[14,27,28] We postulate therefore that the beneficial effects of natriuretic peptides should be brought about, at least in part, by antagonizing local activation and/or action of the RAAS in the kidney.[24–26]

To explore the role of natriuretic peptide/GC-A signaling in aldosterone-induced renal injury, we investigated renal findings of mice deficient in GC-A, along with the challenge of aldosterone and a high-salt diet.

RESULTS

Aldosterone Infusion Causes Accelerated Hypertension in GC-A Knockout Mice

All mice were uninephrectomized and fed with 6% NaCl, with or without aldosterone infusion (0.2 μg/kg body weight per minute) for 4 weeks. Changes in systolic BP (SBP) in each group are shown in Figure 1 (time courses shown in Supplemental Figure 1). Aldosterone infusion in wild-type mice resulted in marginally higher SBP than vehicle (118.1±3.3 versus 116.6±4.5 mmHg at 4 weeks). GC-A knockout mice showed a significantly higher SBP compared with wild-type mice at baseline (126.2±2.7 versus 110.4±3.3 mmHg, $P<0.05$), and revealed marked hypertension after aldosterone infusion compared with vehicle (159.0±6.6 versus 123.0±4.5 mmHg at 4 weeks, $P<0.01$). Administration of hydralazine, spironolactone, or olmesartan in aldosterone-infused GC-A knockout mice resulted in reduced SBP to the same degree (135.7±3.1, 135.2±8.0, and 140.0±5.2 mmHg, respectively). In contrast, there was no significant SBP change with tempol (151.1±6.9 mmHg).

Body and Kidney Weights and Blood Parameters

Body weights and kidney weights are presented in Supplemental Table 1. GC-A knockout mice showed normal kidney weight at baseline but exhibited renal hypertrophy compared with wild-type mice as indicated by an increase in kidney weight per body weight at 4 weeks. Aldosterone infusion caused renal hypertrophy in both wild-type and GC-A knockout mice, and administration of spironolactone ameliorated such changes in GC-A knockout mice.

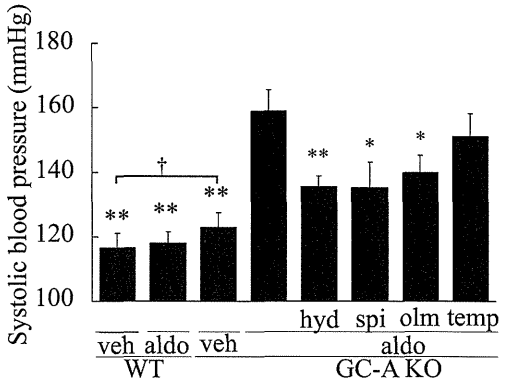

Figure 1. The comparison in SBP at 4 weeks after aldosterone or vehicle infusion. Data are from vehicle-infused wild-type mice (WT veh, n=5), aldosterone-infused wild-type mice (WT aldo, n=8), vehicle-infused GC-A knockout mice (GC-A KO veh, n=5), aldosterone-infused GC-A knockout mice (GC-A KO aldo, n=8), aldosterone-infused GC-A knockout mice treated with hydralazine (KO aldo+hyd, n=6), those treated with spironolactone (KO aldo +spi, n=5), those treated with olmesartan (KO aldo+olm, n=5), and those treated with tempol (KO aldo+temp, n=5). Aldosterone-infused GC-A knockout mice exhibited marked hypertension, and administration of hydralazine, spironolactone, or olmesartan in aldosterone-infused GC-A knockout mice resulted in reduced SBP to the same degree. In contrast, there was no significant SBP change with tempol. *$P<0.05$, **$P<0.01$, versus KO aldo, †$P<0.05$. WT, wild-type; veh, vehicle; aldo, aldosterone; KO, knockout; hyd, hydralazine; spi, spironolactone; olm, olmesartan; temp, tempol.

Serum aldosterone was markedly high (approximately 70-fold) and serum potassium was low in all aldosterone-infused groups (Supplemental Table 1). There was no significant difference in serum aldosterone, potassium, or creatinine levels among aldosterone-infused groups.

Aldosterone Causes Massive Proteinuria in GC-A Knockout Mice

At the basal level (−2 weeks), urinary albumin excretion was not different between wild-type and GC-A knockout mice (38.7±4.9 and 41.4±4.8 μg/mgCr, respectively) (Figure 2A). Aldosterone-infused wild-type mice showed a three-fold increase in urinary albumin excretion at 4 weeks compared with vehicle (129.2±25.4 versus 43.0±6.6 μg/mgCr, $P<0.01$). Surprisingly, aldosterone-infused GC-A knockout mice revealed 260 times higher urinary albumin excretion than vehicle-infused GC-A knockout mice at 4 weeks (17,559±6845 μg/mgCr versus 67.2±24.4 μg/mgCr, $P<0.01$). Administration of hydralazine in these mice significantly reduced BP, but failed to suppress albuminuria (Figure 2B). In contrast, spironolactone administration markedly reduced urinary albumin excretion by 95% in aldosterone-infused GC-A knockout mice (1069±411 μg/mgCr). Moreover, treatment with an angiotensin receptor blocker (ARB) olmesartan significantly reduced urinary albumin excretion by 70% (5450±1765 μg/mgCr). Treatment with tempol also reduced albuminuria by 60% (7125±2292 μg/mgCr). These results suggest that, in the absence of GC-A signaling, aldosterone stimulation can activate the renin-angiotensin system and oxidative stress in the kidney, leading to massive proteinuria.

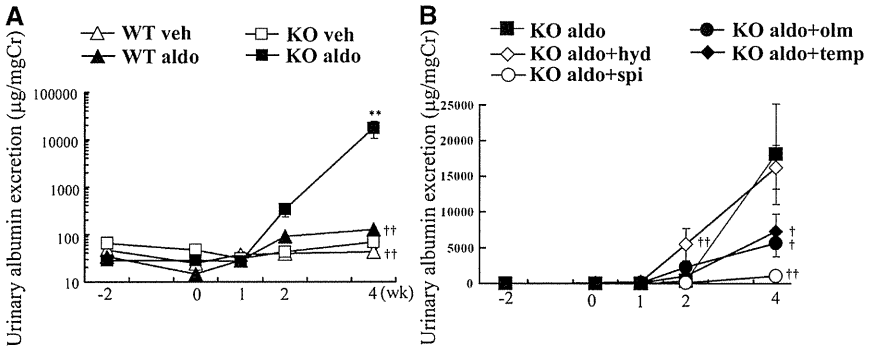

Figure 2. Urinary albumin excretion in wild-type or GC-A knockout mice with or without aldosterone. (A) Aldosterone infusion resulted in a marked increase of albuminuria in GC-A knockout mice. Data from wild-type mice with vehicle (WT veh, open triangles), wild-type mice with aldosterone (WT aldo, filled triangles), GC-A knockout mice with vehicle (KO veh, open squares), and GC-A knockout mice with aldosterone (KO aldo, filled squares) are shown. (B) Administration of spironolactone (spi, open circles), olmesartan (olm, filled circles), or tempol (temp, filled diamonds) significantly reduced albuminuria in aldosterone-infused GC-A knockout mice. Hydralazine (hyd, open diamonds) did not reduce albuminuria. WT veh, $n=5$; WT aldo, $n=8$; KO veh, $n=5$; KO aldo, $n=8$; KO aldo+hyd, $n=6$; KO aldo+spi, $n=5$; KO aldo+olm, $n=5$; and KO aldo+temp, $n=5$. $^{**}P<0.01$, KO veh versus KO aldo, $^{\dagger}P<0.05$, $^{\dagger\dagger}P<0.01$, versus KO aldo.

Renal Histologic Changes in Aldosterone-Infused GC-A Knockout Mice

We examined renal histology at 4 weeks after aldosterone administration. In superficial glomeruli, aldosterone-infused wild-type mice exhibited marginal mesangial expansion with mild glomerular hypertrophy (Figure 3A). Renal histology of GC-A knockout mice showed virtually no significant difference from that of wild-type mice at baseline; after aldosterone infusion, GC-A knockout mice exhibited marked mesangial expansion with glomerular hypertrophy (Figure 3, A and B and Supplemental Figure 2A). Although hydralazine administration failed to ameliorate such changes, treatment with spironolactone, olmesartan, or tempol resulted in inhibited mesangial expansion in these mice.

In juxtamedullary glomeruli, there were minor glomerular abnormalities in aldosterone-infused wild-type mice; in contrast, aldosterone-infused GC-A knockout mice exhibited severe segmental sclerosis and marked glomerular hypertrophy (Figure 3C). Again, these changes were unaltered with hydralazine but were alleviated with spironolactone, olmesartan, or tempol (Figure 3D and Supplemental Figure 2B). The number of sclerotic glomeruli was also significantly reduced with spironolactone, olmesartan, or tempol (Figure 3E). Localization of GC-A was examined by immunohistochemistry. Wild-type mice revealed the presence of GC-A presumably at podocytes, distal tubules, and collecting ducts, which was apparently unaltered with aldosterone infusion (Figure 3F).

We next examined renal fibrotic changes in these mice (Figure 4). Whereas wild-type mice with aldosterone showed slight fibrotic changes with mild tubular atrophy, aldosterone-infused GC-A knockout mice exhibited tubular dilation with marked protein cast deposition and significant tubulointerstitial fibrosis. These changes were not changed with hydralazine but ameliorated with spironolactone, olmesartan, and less effectively with tempol (Figure 4, A and B).

Podocyte Injury in Aldosterone-Infused GC-A Knockout Mice

We then evaluated podocyte injury in these mice. Electron microscopic analyses revealed that wild-type mice with aldosterone exhibited slightly widened podocyte foot processes without thickening of the glomerular basement membrane (GBM) (Figure 5). Vehicle-infused GC-A knockout mice showed thickened GBM without widening of foot processes. GC-A knockout mice with aldosterone showed foot process effacement with irregular thickening of GBM, and these changes were not improved with hydralazine, but reversed with spironolactone and

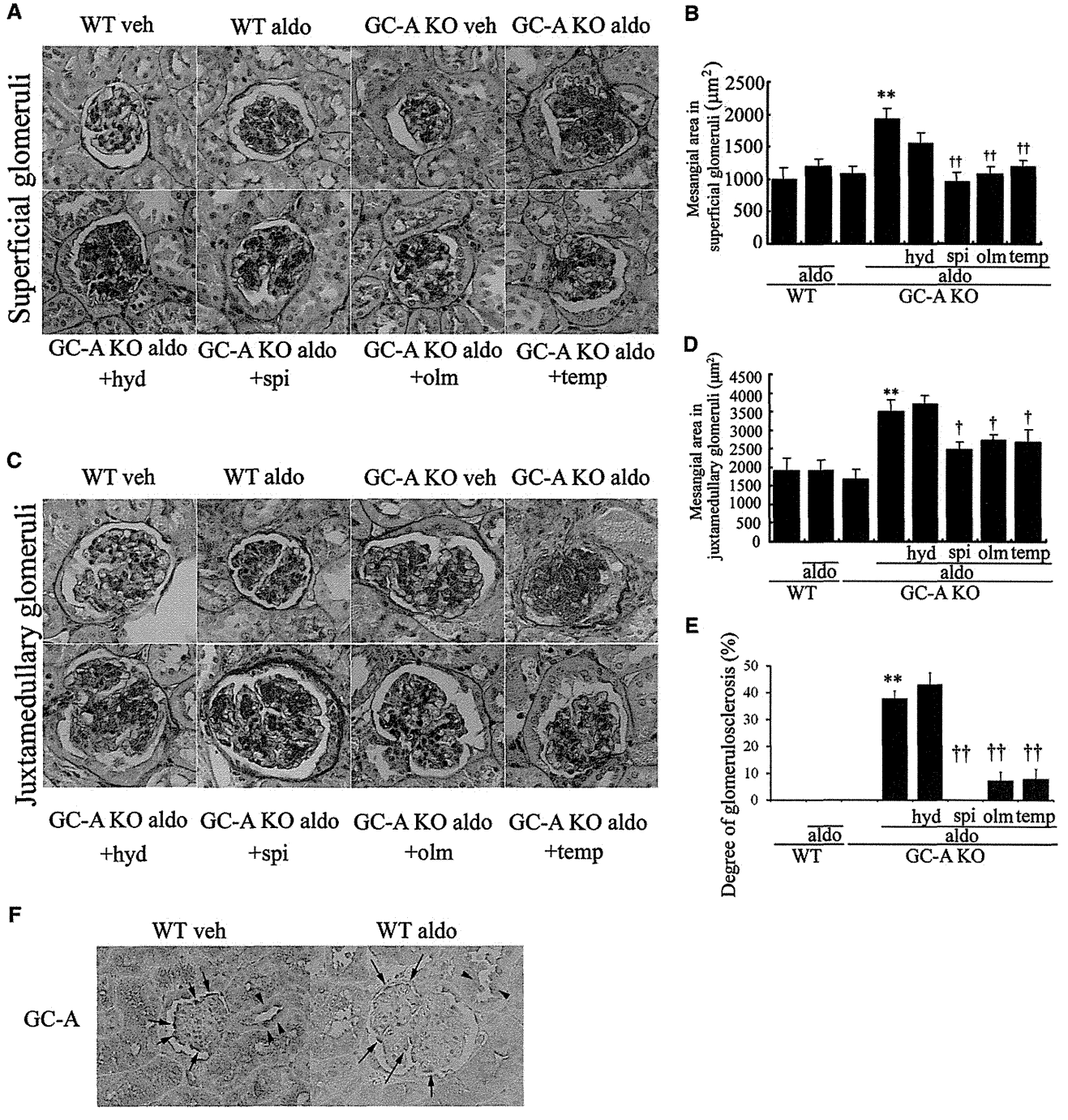

Figure 3. Histologic examination of glomeruli in aldosterone-infused GC-A knockout mice and the localization of GC-A. Light microscopic analyses were performed at 4 weeks after aldosterone administration, stained with periodic acid-Schiff. (A) Representative views of superficial glomeruli. Aldosterone-infused wild-type mice (WT aldo) showed marginal mesangial expansion with mild glomerular hypertrophy. Aldosterone-infused GC-A knockout mice (GC-A KO aldo) exhibited marked mesangial expansion with glomerular hypertrophy. Administration of hydralazine in GC-A knockout mice (GC-A KO aldo+hyd) did not affect glomerular changes. Administration of spironolactone (GC-A KO aldo+spi), olmesartan (GC-A KO aldo+olm), or tempol (GC-A KO aldo+temp) in GC-A knockout mice improved histologic changes. (B) Mesangial area in superficial glomeruli at 4 weeks. (C) Representative views of juxtamedullary glomeruli. Aldosterone-infused GC-A knockout mice showed severe segmental sclerosis and marked glomerular hypertrophy. Administration of spironolactone, olmesartan or tempol ameliorated glomerular changes. (D) Mesangial area in juxtamedullary glomeruli at 4 weeks. (E) Degree of glomerulosclerosis in juxtamedullary glomeruli. (F) Immunohistochemical study for GC-A. GC-A was positive at podocytes (arrows) and distal tubules (arrowheads). WT veh, n=5; WT aldo, n=8; KO veh, n=5; KO aldo, n=8; KO aldo+hyd, n=6; KO aldo+spi, n=5; KO aldo+olm, n=5; and KO aldo+temp, n=5. $^{**}P<0.01$, KO veh versus KO aldo, $^{\dagger}P<0.05$, $^{\dagger\dagger}P<0.01$, versus KO aldo. WT, wild-type; veh, vehicle; aldo, aldosterone; KO, knockout; hyd, hydralazine; spi, spironolactone; olm, olmesartan; temp, tempol.

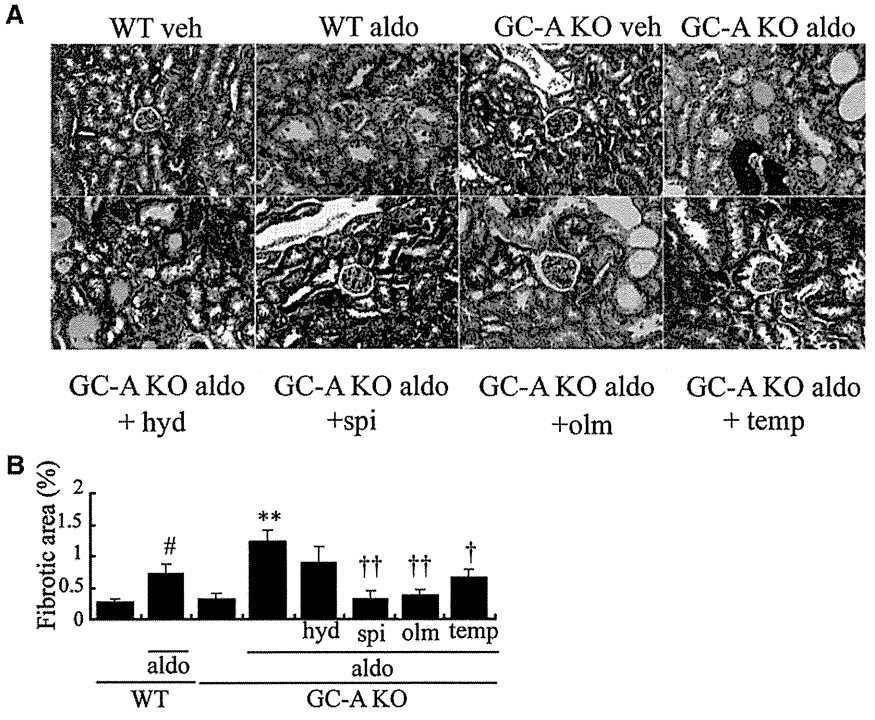

Figure 4. Histologic examination of tubulointerstitial fibrosis by Masson's trichrome-stained sections at 4 weeks. (A) Representative views of tubules and interstitial fibrosis. Aldosterone-infused wild-type mice (WT aldo) showed mild tubulointerstitial fibrosis with tubular atrophy. Aldosterone-infused GC-A knockout mice (GC-A KO aldo) exhibited tubular dilation with protein casts and tubulointerstitial fibrosis. These changes were not improved with hydralazine (GC-A KO aldo+hyd), but ameliorated with spironolactone (GC-A KO aldo+spi), olmesartan (GC-A KO aldo+olm), or tempol (GC-A KO aldo+temp). (B) Fibrotic area at 4 weeks. WT veh, n=5; WT aldo, n=8; KO veh, n=5; KO aldo, n=8; KO aldo+hyd, n=6; KO aldo+spi, n=5; KO aldo+olm, n=5; and KO aldo +temp, n=5. $^{\#}P<0.05$, WT veh versus WT aldo, $^{**}P<0.01$, KO veh versus KO aldo, $^{\dagger}P<0.05$, $^{\dagger\dagger}P<0.01$, versus KO aldo. WT, wild-type; veh, vehicle; aldo, aldosterone; KO, knockout; hyd, hydralazine; spi, spironolactone; olm, olmesartan; temp, tempol.

also lessened with olmesartan (Figure 5, A and B). Tempol administration improved width of foot processes.

The expression of podocyte markers nephrin and podocin was decreased in aldosterone-infused GC-A knockout mice at 4 weeks with or without hydralazine, and such changes were ameliorated with spironolactone, olmesartan, or tempol (Figure 6, A and B).

Gene Expression and ROS in Glomeruli of Aldosterone-Infused GC-A Knockout Mice

Analyses on glomerular expression of extracellular matrix (ECM)–related genes (Figure 7A) revealed that TGF-β1 mRNA was enhanced with aldosterone both in wild-type and in GC-A knockout mice. Such upregulation was significantly reduced with spironolactone or tempol, and tended to decrease with olmesartan treatment. Similar tendency was observed in connective tissue growth factor, fibronectin, and collagen 1 and 4 mRNA expressions (Figure 7A and Supplemental Figure 3).

We next examined the expression of NADPH oxidase 2 (Nox-2) or gp91phox/Cybb, p22phox/Cyba, and Nox-4, which are essential membrane components of NADPH oxidase.[29] Aldosterone infusion upregulated the glomerular expression of gp91phox/Cybb mRNA, and less potently that of p22phox and Nox-4 (Figure 7B and Supplemental Figure 3). Treatment with spironolactone or tempol significantly reduced them. Immunohistochemical study for 8-hydroxydeoxyguanosine (8-OHdG) showed that aldosterone infusion exhibited strong staining mainly at podocytes and tubular cells only in GC-A knockout mice (Figure 7, C and D). Such upregulation was significantly reduced with spironolactone, olmesartan, or tempol, but not with hydralazine.

Enhanced Phosphorylation of MAPKs in Aldosterone-Infused GC-A Knockout Mice

We found a mild increase of phosphorylated extracellular signal-regulated kinase (ERK) in glomeruli of aldosterone-infused wild-type mice (Figure 8A). Phosphorylation of ERK in glomeruli was pronounced in aldosterone-infused GC-A knockout mice. Double immunostaining revealed that the cells expressing phospho-ERK were also positive for Wilms' tumor 1 (WT1), a podocyte marker (Figure 8B). Phosphorylation of ERK was reduced by treatment with spironolactone, olmesartan, or tempol, but not with hydralazine (Figure 8, C and D). Essentially similar results were obtained as to phospho-p38 MAPK-positive cells, which were double stained with WT1 (Figure 8, E and F); the phosphorylation of p38 MAPK was reduced with spironolactone or olmesartan, and also with tempol (Figure 8, E, G, and H).

ANP Inhibits Phosphorylation of ERK and p38 MAPK in Cultured Mouse Podocytes

We examined the effect of ANP on phosphorylation of ERK and p38 MAPK in cultured mouse podocytes. Aldosterone caused the phosphorylation of ERK as quickly as 10 minutes after the stimulation and lasted for as long as 30 minutes (Figure 9A). Pretreatment with ANP completely abolished ERK phosphorylation (Figure 9B). The phosphorylation of p38 MAPK was upregulated at 3 hours after aldosterone stimulation, and such induction was significantly inhibited with ANP treatment (Figure 9, C and D).

GC-A knockdown in podocytes showed higher levels of phosphorylated ERK and p38 MAPK than controls (Supplemental Figure 4). Treatment with olmesartan or spironolactone, but not tempol, partially decreased phospho-ERK; cGMP analog strongly reduced phosphorylation of both ERK and p38 MAPK (Supplemental Figure 4). Cultured podocytes stimulated

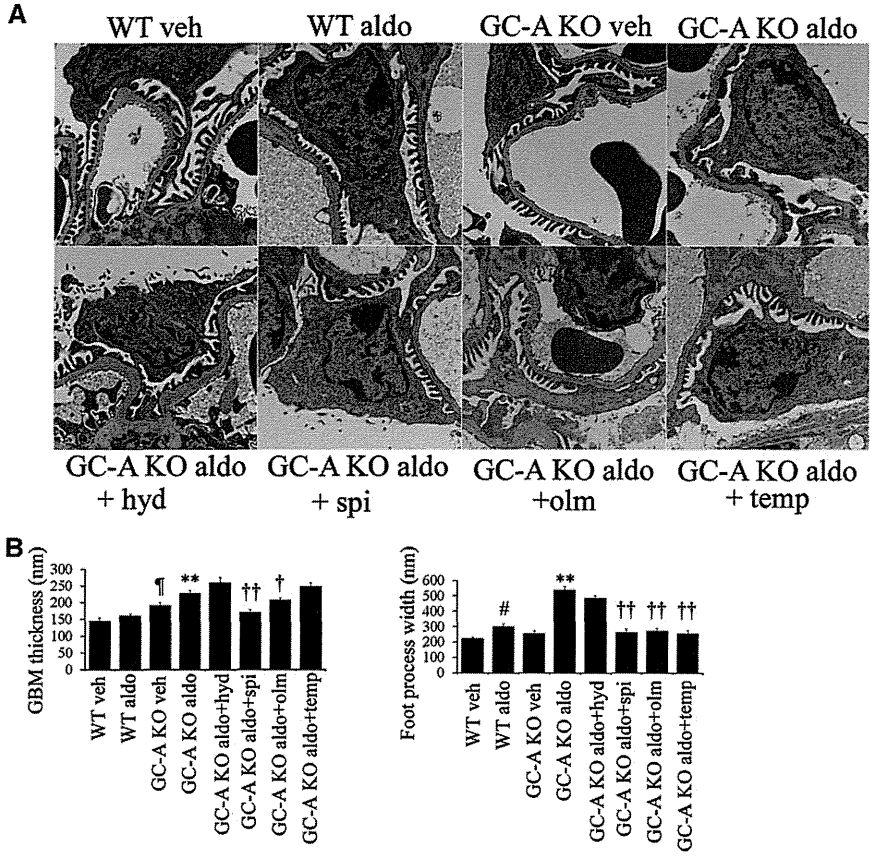

Figure 5. Electron microscopic analyses of glomeruli in aldosterone-infused GC-A knockout mice at 4 weeks. (A) Aldosterone-infused wild-type mice (WT aldo) showed almost normal foot process structure. Vehicle-infused GC-A knockout mice (GC-A KO veh) had normal podocyte foot processes. Aldosterone-infused GC-A knockout mice (GC-A KO aldo) showed foot process effacement with irregular thickening of glomerular basement membrane. These changes were not improved with administration of hydralazine (GC-A KO aldo+hyd), but ameliorated with spironolactone (GC-A KO aldo+spi), olmesartan (GC-A KO aldo+olm), or tempol (GC-A KO aldo+temp). (B) GBM thickness and foot process width (n=3, each). $^{\#}P<0.05$, WT veh versus WT aldo, $^{**}P<0.01$, KO veh versus KO aldo, $^{\dagger}P<0.05$, $^{\dagger\dagger}P<0.01$, versus KO aldo, $^{\P}P<0.05$, KO veh versus WT veh. WT, wild-type; veh, vehicle; aldo, aldosterone; KO, knockout; hyd, hydralazine; spi, spironolactone; olm, olmesartan; temp, tempol.

with aldosterone upregulated expression of connexin43 (Gja1), a podocyte injury marker. This upregulation was significantly inhibited by the treatment with MAPK kinase (MEK) inhibitor U0126 or p38 MAPK inhibitor SB203580 (Figure 9E). Finally, we confirmed whether aldosterone action was mediated through a mineralocorticoid receptor. Upregulation of connexin43 mRNA in aldosterone-stimulated podocytes was not reduced by glucocorticoid receptor blocker mifepristone, but by spironolactone (Figure 9F).

DISCUSSION

We investigated the role of the natriuretic peptide/GC-A system in aldosterone-induced renal injury. Although aldosterone administration in wild-type mice resulted in minor glomerular abnormalities with marginal increase of albuminuria, GC-A–deficient mice exhibited accelerated hypertension and severe glomerulopathy with massive proteinuria, indicating that GC-A signaling should normally act to inhibit aldosterone-induced glomerular injury. We must be cautious to interpret BP by tail-cuff manometry, because it is not as precise as direct monitoring. Nevertheless, these actions were not merely BP dependent, and we therefore hypothesized that GC-A signaling works at podocytes in this model. In fact, aldosterone exerted marked podocyte injury, only in the absence of GC-A.

Besides massive proteinuria, aldosterone caused glomerulosclerosis and interstitial fibrosis in a mineralocorticoid receptor-dependent fashion (Figures 2–4). Spironolactone treatment with modest BP reduction (Figure 1) almost completely abolished these abnormalities, suggesting that aldosterone acts perhaps via the receptor on the podocytes and mesangium in addition to that in tubules.[7–9,11–13] To note, an ARB olmesartan markedly ameliorated proteinuria and glomerular/podocyte injuries (Figures 2–6), suggesting that aldosterone activation of the RAAS in the kidney may have a causative role, especially in the absence of GC-A signaling. Several studies have provided evidence for positive feedback between aldosterone and the RAAS,[5–7] and GC-A knockout mice showed augmented angiotensin-converting enzyme and AT1 mRNA expression.[30] Activated AT1 signaling at podocytes would be sufficient to cause proteinuria and glomerular injury.[31,32] Furthermore, the crosstalk between AngII and GC-A signaling was shown in cultured podocytes.[33] These data suggest that lack of GC-A in the kidney should have a critical role in exaggerated activation of the "local" RAAS, which was abrogated by ARB treatment.

Aldosterone increases ROS production in the kidney.[7,8,12] This study reveals that the glomerular expression of gp91phox, a prototype of Nox family,[29] was upregulated in aldosterone-infused GC-A knockout mice (Figure 7). Treatment with tempol, a membrane-permeable radical scavenger,[8] inhibited such increases together with significant amelioration in nephropathy (Figures 2–6), suggesting the importance of ROS in this model. Thus far, little is known on the relationship between natriuretic peptides and ROS in renal injury. It has been reported that ANP counteracts ROS generation in aortic smooth muscle cells,[34] and inhibits ROS-induced cell damage

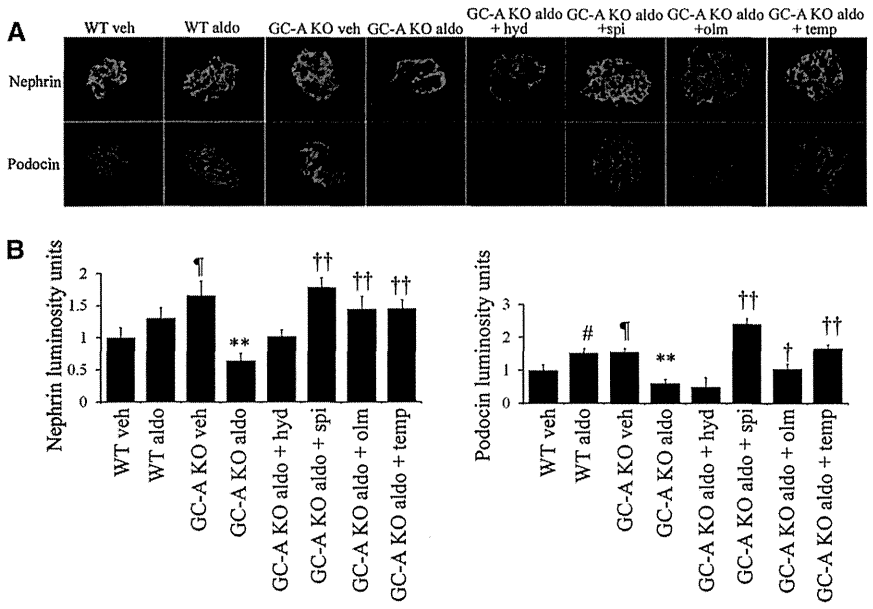

Figure 6. Immunostaining for nephrin and podocin. (A) Aldosterone-infused wild-type mice (WT aldo) showed normal linear staining for nephrin and podocin. Aldosterone-infused GC-A knockout mice (GC-A KO aldo) exhibited decreased expression of nephrin and podocin at 4 weeks. The expression of both nephrin and podocin was recovered by administration with spironolactone (GC-A KO aldo+spi), olmesartan (GC-A KO aldo+olm), or tempol (GC-A KO aldo+temp), but not with hydralazine (GC-A KO aldo+hyd). (B) Quantification of the mean intensity and the area of fluorescent staining for nephrin and podocin, and the products of multiplying the intensity and the area are shown. WT veh, n=5; WT aldo, n=8; KO veh, n=5; KO aldo, n=8; KO aldo+hyd, n=6; KO aldo+spi, n=5; KO aldo+olm, n=5; and KO aldo+temp, n=5. #$P<0.05$, WT veh versus WT aldo, **$P<0.01$, KO veh versus KO aldo, $^{\dagger}P<0.05$, $^{\dagger\dagger}P<0.01$, versus KO aldo, $^{\P}P<0.05$, KO veh versus WT veh. WT, wild-type; veh, vehicle; aldo, aldosterone; KO, knockout; hyd, hydralazine; spi, spironolactone; olm, olmesartan; temp, tempol.

via the GC-A/cGMP pathway.[35] The role of ROS in renal injury has been extensively studied,[36] and redox control is crucial in the pathophysiology of human and rodent diabetic nephropathy.[37,38] In this study, aldosterone caused increased glomerular expression of ROS- and ECM-related genes both in knockout and control mice. However, augmented 8-OHdG, massive proteinuria, and fibrotic changes occurred only in GC-A knockout mice, suggesting that, in wild-type mice, GC-A signaling may hamper intracellular mechanisms downstream of ROS signal against disease progression.

ROS-induced cell injury is mediated in part by the activation of MAPKs.[8,9] p38 MAPK plays a critical role in inflammation,[39] cytoskeleton stability,[40] and podocyte function.[41] We previously showed that inhibition of p38 MAPK markedly ameliorates podocyte injury and proteinuria in rodent models of nephrotic syndrome.[41] In this study, knockout mice with aldosterone exhibited augmented phosphorylation of p38 MAPK in podocytes, which was inhibited by RAAS blockade as well as tempol (Figure 8). In addition, ANP suppressed p38 MAPK phosphorylation, which was increased by GC-A knockdown in cultured podocytes (Figure 9, Supplemental Figure 4). Moreover, upregulation of connexin43, one of the earliest podocyte injury markers,[42] was induced by aldosterone and reduced by p38 MAPK inhibition (Figure 9E). It is thus conceivable that GC-A deficiency facilitated aldosterone- and ROS-induced activation of p38 MAPK, causing pronounced podocyte damage. It has been reported that ANP inhibits ROS-mediated p38 MAPK activation in lung endothelial cells.[43]

This study also demonstrated the enhanced ERK phosphorylation at podocytes in aldosterone-infused GC-A knockout mice, which was attenuated with RAAS blockade. We previously showed that natriuretic peptides prevent glomerular ERK activation in anti-GBM GN[25] and ameliorate AngII-induced cardiac hypertrophy and fibrosis.[44] *In vitro*, ANP and cGMP analog inhibited aldosterone-induced ERK phosphorylation (Figure 9), suggesting that natriuretic peptide/GC-A/cGMP pathway can counteract the activation of both MAPK pathways (Supplemental Figure 5).

This study provides an idea that suppression of GC-A signaling would be a potential risk for proteinuria under high aldosterone state. Impaired GC-A signaling can often be seen in chronic heart failure (natriuretic peptide resistance), in which RAAS activation would inevitably occur both systemically and locally.[45] Such conditions are well recognized as potentially harmful to the kidney, and supplementation of ANP or BNP could become a therapeutic option against disease progression.

In summary, this study reveals that aldosterone causes massive proteinuria and podocyte injury in the absence of GC-A signaling with the activation of ROS and MAPKs, and that RAAS blockade and ROS inhibition could ameliorate these abnormalities. These findings suggest that local inhibition of the RAAS and oxidative stress in podocytes may be a novel mechanism involved in the pleiotropic and renoprotective properties of endogenous natriuretic peptide/GC-A system.

CONCISE METHODS

Reagents and Antibodies

Aldosterone was obtained from Sigma Aldrich (St. Louis, MO). Reagents used were hydralazine (Sigma Aldrich), spironolactone (Sigma Aldrich), olmesartan (a gift from Daiichi Sankyo Pharmaceutical, Tokyo, Japan), tempol (Sigma Aldrich), MEK inhibitor U0126 (Cell Signaling Technology, Boston, MA), p38 MAPK inhibitor SB203580 (Cell Signaling Technology), and glucocorticoid receptor blocker mifepristone (Sigma Aldrich). Primary antibodies used for

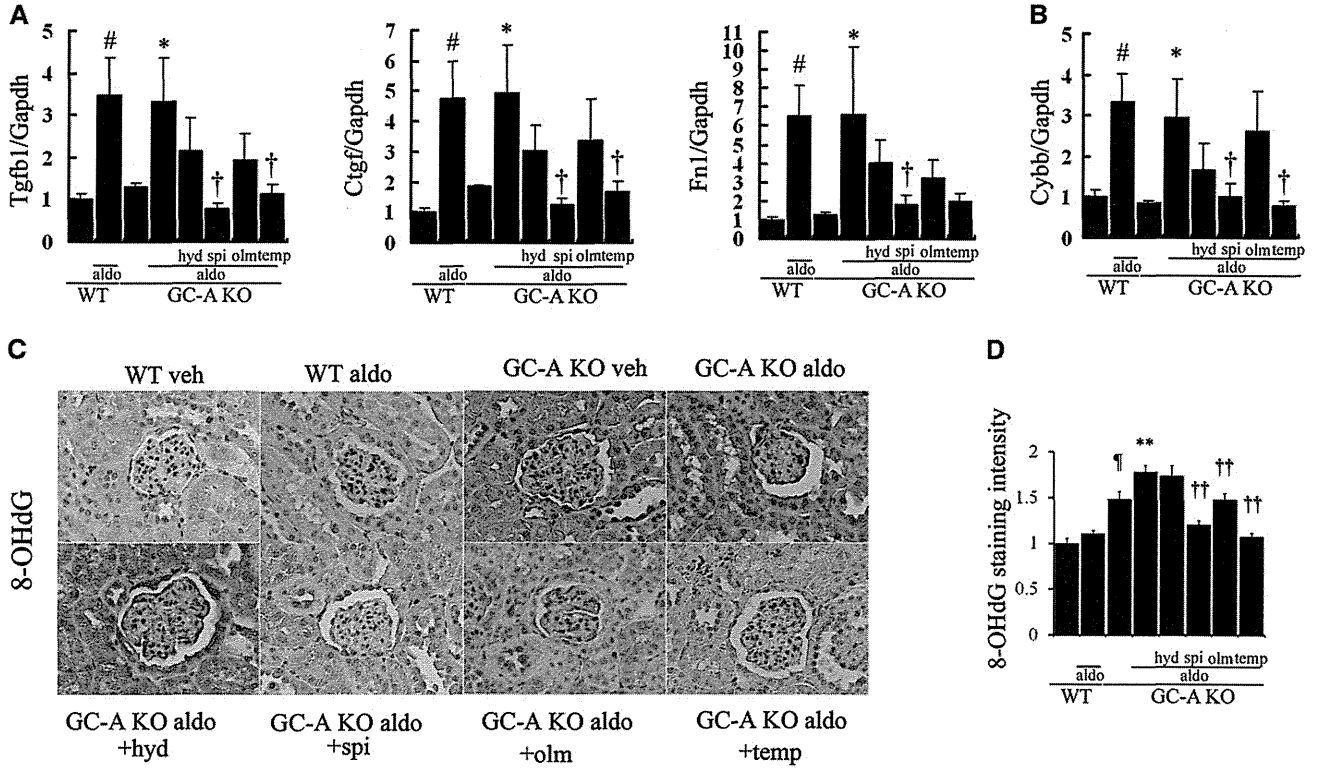

Figure 7. Glomerular mRNA expression at 4 weeks after aldosterone administration and ROS. (A, B) Real-time RT-PCR analyses of TGF-β1 (Tgfb1), connective tissue growth factor (Ctgf), fibronectin (Fn1), and gp91phox (Cybb) are shown. GAPDH mRNA expression is used as the control. (C) Immunohistochemical study for 8-OHdG. Aldosterone-infused wild-type mice (WT aldo) did not show the increase of 8-OHdG. Strong staining of 8-OHdG was detected in vehicle-infused GC-A knockout mice (GC-A KO veh), and aldosterone infusion (GC-A KO aldo) augmented 8-OHdG staining mainly at podocytes and tubular cells. Staining of 8-OHdG was reduced by administration with spironolactone (GC-A KO aldo+spi), olmesartan (GC-A KO aldo+olm), or tempol (GC-A KO aldo+temp), but not with hydralazine (GC-A KO aldo+hyd). (D) Quantification of the mean intensity of staining for 8-OHdG. WT veh, n=5; WT aldo, n=8; KO veh, n=5; KO aldo, n=8; KO aldo+hyd, n=6; KO aldo+spi, n=5; KO aldo+olm, n=5; and KO aldo+temp, n=5. $^{\#}P<0.05$, WT veh versus WT aldo,$^{*}P<0.05$, $^{**}P<0.01$, KO veh versus KO aldo, $^{\dagger}P<0.05$, $^{\dagger\dagger}P<0.01$, versus KO aldo, $^{\P}P<0.05$, KO veh versus WT veh. WT, wild-type; veh, vehicle; aldo, aldosterone; KO, knockout; hyd, hydralazine; spi, spironolactone; olm, olmesartan; temp, tempol.

Western blotting and immunohistochemical studies were goat anti-nephrin (R&D Systems, Minneapolis, MN), rabbit anti-podocin (Sigma Aldrich), rabbit anti-p44/42 MAPK, rabbit anti-phospho-p44/42 MAPK, rabbit anti-p38 MAPK, rabbit anti-phospho-p38 MAPK (Cell Signaling Technology), and goat anti-8-OHdG (Millipore, Temecula, CA) antibodies.

Animal Experiments

All animal experiments were approved by the Animal Experimentation Committee of Kyoto University Graduate School of Medicine. Mice deficient in GC-A were produced on 129/SVJ background[19] and then backcrossed with C57BL/6J mice more than 10 times. Male GC-A knockout mice or their wild-type littermates (approximately 28 g) received a left uninephrectomy or sham operation under intraperitoneal pentobarbital anesthesia (at −2 weeks). At 2 weeks after uninephrectomy or sham operation, an osmotic minipump (model 2004; Alzet, Cupertino, CA) was implanted subcutaneously to infuse vehicle or aldosterone (at 0 weeks). All mice were fed a diet containing 6% NaCl. Mice were assigned randomly to treated or untreated groups for 4 weeks: group 1, vehicle (2% ethanol)–infused wild-type mice (n=5); group 2, aldosterone (0.2 μg/kg body weight per minute)–infused wild-type mice (n=8); group 3, vehicle-infused GC-A knockout mice (n=5); group 4, aldosterone-infused GC-A knockout mice (n=8); group 5, aldosterone-infused GC-A knockout mice with hydralazine (60 mg/kg per day, in drinking water) (n=6); group 6, aldosterone-infused GC-A knockout mice with spironolactone (30 mg/kg per day, in drinking water) (n=5); group 7, aldosterone-infused GC-A knockout mice with olmesartan (10 mg/kg per day, in drinking water) (n=5); and group 8, aldosterone-infused GC-A knockout mice with tempol (110 mg/kg per day, in drinking water) (n=5).

Animals were given water *ad libitum*. BP was measured in conscious mice by the tail-cuff method (MK-2000ST; Muromachi Kikai, Tokyo, Japan) at −2, 0, 1, 2, and 4 weeks.[25] For urine measurements, each animal was housed separately in a metabolic cage (Shinano Manufacturing, Tokyo, Japan) at −2, 0, 1, 2, and 4 weeks.[46] Blood and kidney samples were harvested at 4 weeks. Glomeruli were isolated by the graded sieving method.[46] Urinary and serum creatinine were measured by the enzymatic method (SRL, Tokyo, Japan).[46] Serum aldosterone was measured by RIA (SRL). Urinary albumin excretion was assayed with a murine albumin ELISA kit (Exocell, Philadelphia, PA).[46]

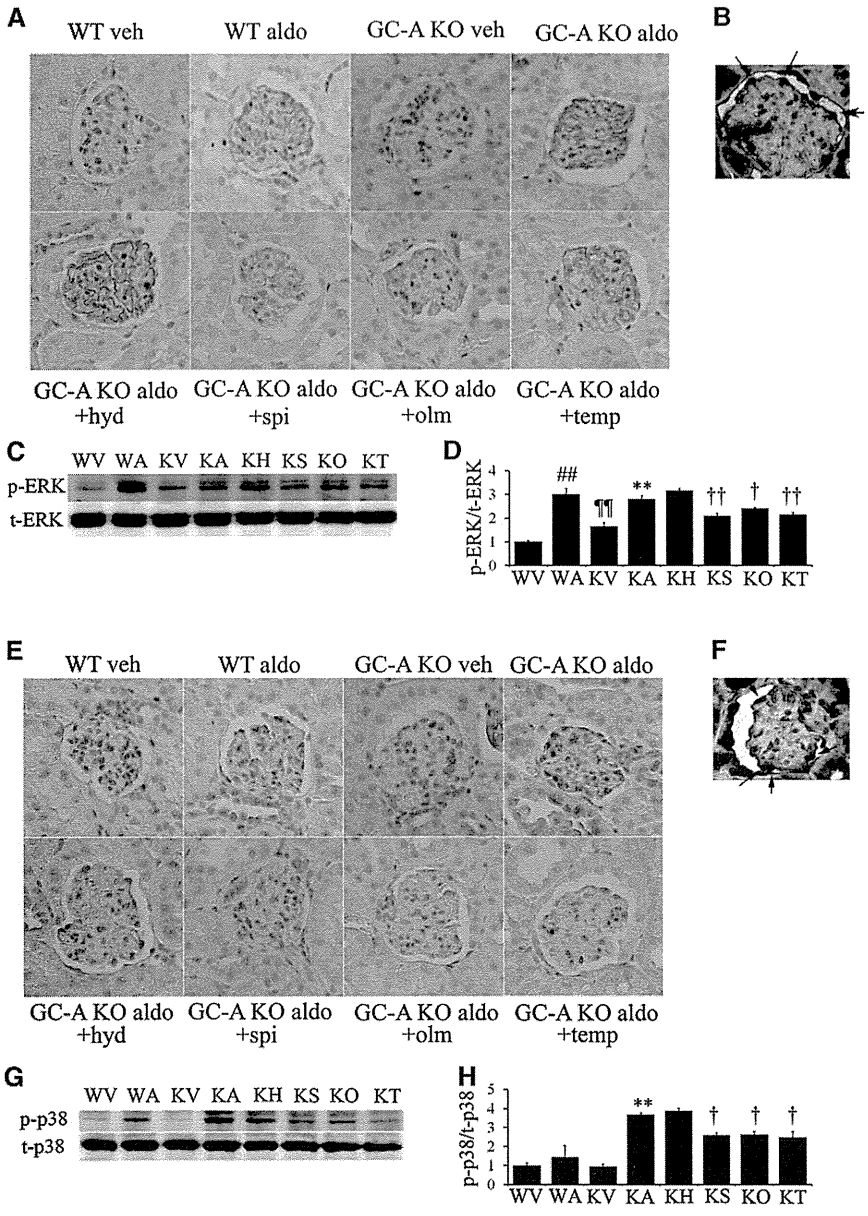

Figure 8. Enhanced phosphorylation of ERK and p38 MAPK in glomeruli of aldosterone-infused GC-A knockout mice. (A) Immunohistochemical study for phospho-ERK at 4 weeks after aldosterone infusion. (B) Double immunostaining for phospho-ERK (brown) and Wilms' tumor 1 (WT1, blue). Arrows indicate double positive cells. (C) Western blotting for phospho-ERK and total ERK in glomeruli of mice. (D) Quantification of relative phospho-ERK to total ERK levels analyzed with densitometer. (E) Immunohistochemical study for phospho-p38 MAPK at 4 weeks after aldosterone infusion. (F) Double immunostaining for phospho-p38 MAPK (brown) and WT1 (blue). Arrows indicate double positive cells. (G) Western blotting for phospho-p38 MAPK and total p38 MAPK in glomeruli of mice. (H) Quantification of relative phospho-p38 MAPK to total p38 MAPK levels analyzed with densitometer. n=3, each. $^{\#\#}P<0.01$, WT veh versus WT aldo, $^{**}P<0.01$, KO veh versus KO aldo, $^{\dagger}P<0.05$, $^{\dagger\dagger}P<0.01$, versus KO aldo, $^{¶¶}P<0.01$, KO veh versus WT veh. WT, wild-type; veh, vehicle; aldo, aldosterone; KO, knockout; hyd, hydralazine; spi, spironolactone; olm, olmesartan; temp, tempol; WV, wild-type mice with vehicle; WA, wild-type mice with aldosterone; KV, GC-A KO mice with vehicle; KA, GC-A KO mice with aldosterone; KH, GC-A KO mice with aldosterone treated with hydralazine; KS, GC-A KO mice with aldosterone treated with spironolactone; KO, GC-A KO mice with aldosterone treated with olmesartan; KT, GC-A KO mice with aldosterone treated with tempol.

Renal Histology and Electron Microscopy

Histologic and electron microscopic examinations were performed as described previously.[46,47] Briefly, kidney sections stained with periodic acid–Schiff were examined by light microscopy (IX-81; Olympus, Tokyo, Japan). The cross-sectional area and the mesangial area in both 10 superficial and 10 juxtamedullary glomeruli were measured quantitatively using a computer-aided manipulator (MetaMorph software; Molecular Devices, Sunnyvale, CA).[46] The number of sclerotic and all juxtaglomerular glomeruli was counted. The fibrotic area was also measured in Masson's trichrome-stained kidney sections quantitatively using a computer-aided manipulator (MetaMorph software).[47] Electron microscopic examination was performed in an electron microscope (H-7600; Hitachi, Tokyo, Japan). GBM thickness and foot process width were measured with Image J software (http://rsbweb.nih.gov/ij/; n=3, each). These procedures were performed by two investigators blinded to the origin of the slides and photos, and the mean values were calculated.

Immunohistochemistry

Immunofluorescence analyses for nephrin and podocin were described previously.[41,46] Briefly, cryostat sections were incubated with goat anti-nephrin antibody or rabbit anti-podocin antibody, and then incubated with FITC-labeled secondary antibodies (Jackson ImmunoResearch, West Grove, PA). Positive area and mean fluorescent intensity were measured with Image J software (n=3, each). Immunohistochemical studies for phospho-ERK, phospho-p38 MAPK, and 8-OHdG were also performed as previously described.[41] Briefly, paraffin-embedded sections were incubated with rabbit anti-phospho-p44/42 MAPK (ERK) antibody, rabbit anti-phospho-p38 MAPK antibody, or goat anti-8-OHdG antibody, and then incubated with horseradish peroxidase–labeled anti-rabbit or anti-goat antibodies (Jackson ImmunoResearch). Mean staining intensity was measured with Image J software (n=3, each). The sections were developed with 3,3′-diaminobenzidine tetrahydrochloride. WT1 immunostaining was performed as described.[46] For immunohistochemical studies for GC-A, paraffin-embedded, autoclave-heated sections were treated with 3% H_2O_2 and a biotin blocking kit (Vector Laboratories, Burlingame, CA), and were incubated with 10% normal goat serum in

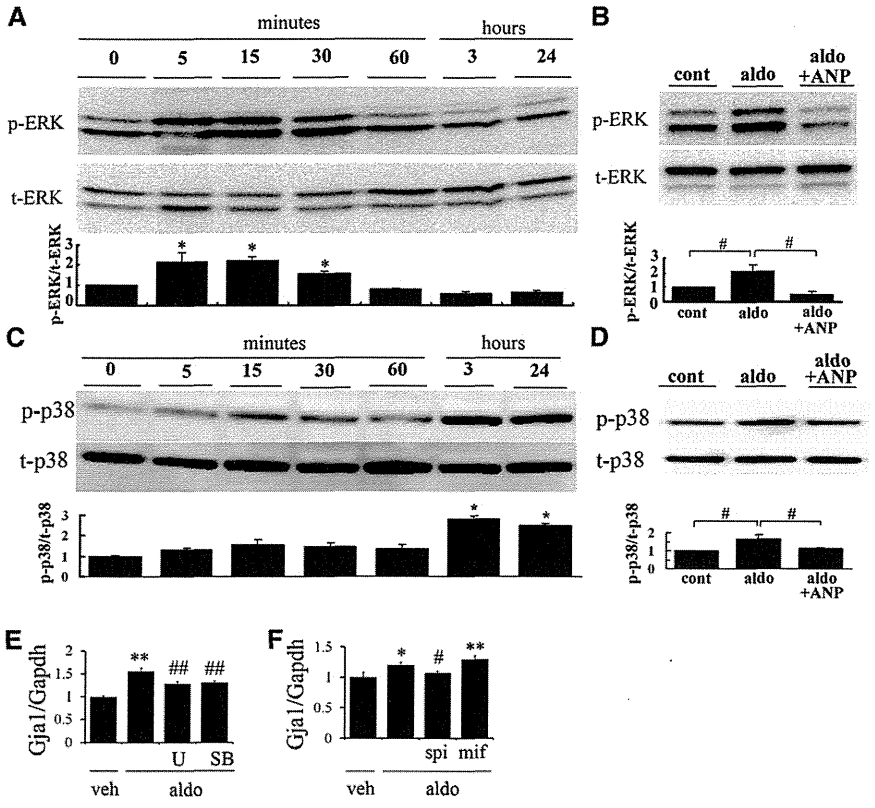

Figure 9. Aldosterone-induced phosphorylation of ERK and p38 MAPK in cultured mouse podocytes. (A) Time course of phospho-ERK and total ERK protein after administration of aldosterone (1 μM) in cultured podocytes. *P<0.01, versus 0 minutes. n=5. (B) Inhibitory effects of ANP (1 μM) on aldosterone-induced ERK phosphorylation. ANP (aldo+ANP) or vehicle (aldo) was administered 30 minutes before aldosterone or vehicle (cont) stimulation (1 μM). Cells were harvested at 10 minutes after aldosterone stimulation. #P<0.01. n=5. (C) Time course of phospho-p38 MAPK and total p38 MAPK protein after administration of aldosterone (1 μM) in cultured podocytes. *P<0.01, versus 0 minutes. n=5. (D) Inhibitory effects of ANP (1 μM) on aldosterone-induced p38 MAPK phosphorylation at 3 hours. Mean ± SEM *P<0.01, versus 0 minutes. #P<0.01. n=5. *P<0.01, versus 0 minutes. #P<0.01. n=5. (E) Inhibitory effects of MEK inhibitor or p38 MAPK inhibitor on connexin43 (Gja1) mRNA expression in mouse podocytes. U. U0126 (10 μM); SB, SB203580 (10 μM). **P<0.01 versus veh. ##P<0.01 versus aldosterone. n=3. (F) Glucocorticoid receptor blocker, mifepristone, did not reduce aldosterone-induced connexin43 expression. Spi, spironolactone (10 μM), mifepristone (10 μM). *P<0.05, **P<0.01 versus veh, #P<0.05 versus aldosterone. n=3. WT, wild-type; veh, vehicle; aldo, aldosterone; KO, knockout; hyd, hydralazine; spi, spironolactone; olm, olmesartan; temp, tempol.

PBS. The sections were incubated with rabbit anti-NPR-A (GC-A) antibody (Santa Cruz Biotechnology, Santa Cruz, CA) diluted 1:20 in PBS for 1 hour at room temperature, and then incubated with goat biotin-conjugated anti-rabbit antibody (Vector Laboratories). The sections were processed with LSAB2 streptavidin-HRP (DAKO, Glostrup, Denmark), and developed with 3,3′-diaminobenzidine tetrahydrochloride.

Glomerular RNA Extraction and Real-Time RT-PCR Analyses

Quantitative real-time RT-PCR was performed using the StepOnePlus system (Applied Biosystems, Foster City, CA) as described previously.[46] TGF-β1, COL1A1, COL4A3, fibronectin, gp91phox/Cybb (Nox-2), p22phox/Cyba, and Nox-4 mRNA expressions were evaluated. Some of primers and probe sets were described elsewhere[46] and included the following: COL1A1 forward primer, 5′-gtcccaacccccaaagac-3′; COL1A1 reverse primer, 5′-catcttctgag-tttggtgatacgt-3′; COL1A1 probe, 5′-FAM-tgctgtgctttctgcccgga-TAMRA-3′; Cybb forward primer, 5′-ggtgacaatgagaacgaagagtatc-3′; Cybb reverse primer, 5′-gagacacagtgtgatgacaattcc-3′; Cybb probe, 5′-FAM-cagccaaccgagtcacggccaca-tac-TAMRA-3′; Cyba forward primer, 5′-cccctcaccaggaattactacg-3′; Cyba reverse primer, 5′-cactgctcacctcggatgg-3′; Cyba probe, 5′-FAM-ctccacttcctgttgtcggtgcctgc-TAMRA-3′; Nox-4 forward primer, 5′-gcaagactctacacatcacatgtg-3′; Nox-4 reverse primer, 5′-tgctgcattcagttcaag-gaaatc-3′; Nox-4 probe, 5′-FAM-tctcaggtgtg-catgtagccgccca-TAMRA-3′; Gja1 forward primer, 5′-ctctccttttccttgacttcagc-3′; Gja1 reverse primer, gaccttgtccagcagcttcc; and Gja1 probe, 5′-FAM-aaggagttccaccactttggcgtgcc-TAMRA-3′. Expression of each mRNA was normalized with GAPDH mRNA (TaqMan rodent GAPDH control reagents; Applied Biosystems).

Cell Cultures

A conditionally immortalized mouse podocyte cell line was provided by Dr. Peter Mundel (University of Miami Miller School of Medicine, Miami, FL) and cultured as described.[41] For time-course experiments, differentiated podocytes were made quiescent in medium that contained 0.1% FBS for 24 hours, and then cells were stimulated with 1 μM aldosterone and further incubated for a period ranging from 5 minutes to 24 hours. The effect of ANP (Peptide Institute, Osaka, Japan) on phosphorylation of ERK and p38 MAPK was studied in the presence of aldosterone. Cells were made quiescent in medium that contained 0.1% FBS for 24 hours, pretreated with 1 μM ANP or vehicle (final 0.005% glucose solution) 30 minutes before stimulation with 1 μM aldosterone or vehicle (final 0.2% ethanol), and then harvested at 10 minutes or 3 hours after stimulation for ERK and p38 MAPK analyses, respectively.

Connexin43 (Gja1) mRNA expression was evaluated by TaqMan PCR. Differentiated podocytes were made quiescent, pretreated with 10 μM U0126 or 10 μM SB203580 for 30 minutes, and then stimulated with 1 μM aldosterone. Cells were harvested at 24 hours after stimulation with a RNeasy Mini kit (Qiagen). For analysis of the glucocorticoid pathway, cells were pretreated with 10 μM mifepristone or 10 μM spironolactone and were harvested at 3 hours after aldosterone (1 μM) stimulation.